Reply to Anonymous Referee #1 for Climatic Impacts of Stratospheric Geoengineering with Sulfate, Black Carbon and Titania Injection

We thank the anonymous reviewer for their detailed comments and suggestions relating to the paper. In our response, we aim to address each of the reviewer's comments and make the corresponding changes to the manuscript where necessary (red indicates sentences removed, blue indicates sentences added).

Specific responses

1. Abstract - The reviewer notes that the following statement is too strong:
    As injection rates for titania are close to those for sulfate, there appears to be little benefit of using titania when compared to the injection of sulfur dioxide
    In response, we amend the statement to the following:
    As injection rates and climatic impacts for titania are close to those for sulfate, there appears to be little benefit in terms of climatic influence of using titania when compared to the injection of sulfur dioxide
    The amended statement takes into account that the conclusion is relevant with respect to the climatic impacts of titania and sulfate injection. We do not feel that it is necessary to discuss the possible non-climatic impacts in the abstract as the suitable caveats concerning their exclusion in this investigation are given in the results section.

2. Introduction – The reviewer questions why we chose RCP8.5 as a baseline scenario. We have explained why we chose RCP8.5 in the following sentence, which is on P30046.
    RCP8.5 is selected to give a significant greenhouse effect against which to employ geoengineering, in order to distinguish the climatic impacts specific to each aerosol
    We appreciate however that the choice of RCP8.5 over the more societally-optimistic RCP4.5 scenario is slightly-controversial (and novel) and will affect the findings of this report. In particular, the aerosol injection rates, deposition rates, mass concentrations and the magnitude of stratospheric changes would all be different with a baseline RCP4.5 scenario. We modify the introduction as follows.
    RCP8.5, which is the high-end carbon-intensive CMIP5 scenario, is selected to give a significant greenhouse effect against which to employ geoengineering, in order to distinguish the climatic impacts specific to each aerosol. Observations have shown that the current global GHG emissions exceed the emissions inherent in RCP8.5 [Peters et al, 2013]; therefore our work could be considered as geoenineering against a business-as-usual scenario. Additionally, the next generation of GeoMIP simulations (GeoMIP6) will utilise a carbon-intensive scenario [Kravitz et al, 2015], hence our work will provide a useful supplement to those results.
    Also, in section 5, we have added the following paragraph to discuss the possible differences if RCP4.5 had been used.

The climatic impacts described in section 4 are specific to geoengineering against a baseline RCP8.5 scenario. If instead we had used a middle-of-the-road GHG-concentrations scenario such as RCP4.5 [Taylor et al., 2012], as used in the first tier of GeoMIP scenarios [Kravitz et al., 2011], then less aerosol-injection would be needed to obtain TOA-Imb=0 and therefore the aerosol deposition rates and atmospheric mass concentrations would be less than those reported in section 4. One would expect that the magnitude of stratospheric temperature changes (fig. 8) and therefore zonal-mean zonal wind changes (fig. 12) would be much less for each of the aerosols, possibly confounding the conclusions giving here relating to their comparative efficacy. An estimate for the amount of SAI required for RCP4.5 can be garnered from integrating the temperature anomalies for RCP8.5 and RCP4.5 for the period 2020-2100. The ratio of the integrated temperature anomalies for RCP4.5 to RCP8.5 is 0.43, hence we can assume that the injection rates required for RCP4.5 are ~0.43 of those for RCP8.5, producing a climate perturbation ~0.43 times as great. A further set of simulations, which instead utilise RCP4.5 as the baseline scenario, would be required to test this hypothesis.

3. Figure 1 – The reviewer questions the discontinuities between the short wave and long wave points in figure 1. The discontinuities between the short wave and long wave points in figure 1 are not due to uncertainty in the optical properties. Rather, the wavelength at which the points are plotted is the average wavelength of the spectral waveband used in the model. There are 5 disparate wavebands in the short wave spectrum and 9 wavebands in the long wave. In the short wave, the wavebands used for this experiment are 0.2-0.32, 0.32-0.69, 0.69-1.19, 1.19-2.38, and 2.38-10 μm. In the long wave, the wavebands used are 3.34-6.67, 6.67-7.52, 7.52-8.33, 8.93-10.1, 8.33-12.5, 13.3-16.9, 12.5-18.1, 18.1-25, 25-10000 μm. It is then clear that the average-wavelengths of the wavebands of the two spectrums overlap (max SW = 6.19 μm, min LW = 5 μm), which explains the disparity in figure 1. The equivalent image from Ferraro et al (2011) – their figure 1 – shows the same discontinuities between the short wave and long wave bands, which is because both our models (their FDH code, our HadGEM2-CCS) use the Edwards and Slingo radiation code (ES96) and we both evaluate the optical constants at the same wavebands [Edwards and Slingo, 1996]. We appreciate that this point was not made clear in the article and could cause confusion to a reader. Therefore we amend the caption in figure 1 as follows.
   *"**Figure 1.** Optical properties as a function of wavelength for a) accumulation-mode sulfate, b) titania, c) black carbon. Points are plotted at the middle of each spectral waveband, as detailed in Bellouin et al (2007)"*

4. Figure 1 & figure 10 – The reviewer questions why we get different results to Ferraro et al (2011). There are many differences between the models and configurations used by ourselves and Ferraro et al (2011), hereafter F11, which could contribute to the different stratospheric temperature perturbations. We will concentrate on sulfate and titania, as black carbon is similar between the two, and give possible reasons for the

temperature-change differences. We will then summarise these for addition to the article.

- a. The first point is that F11 use a fixed dynamical heating (FDH) code and not a dynamical-model; their code doesn't take into account feedback from changes in the atmospheric and oceanic circulation, sea surface temperatures, etc as HadGEM2-CCS will. Also their model has 38 vertical levels up to 40 km altitude rather than the 60 vertical levels up to 85 km in our model

- b. The second point is that we use inherently different climatologies, which include different ozone, baseline stratospheric temperatures, greenhouse gases, clouds, etc. All of which will contribute to the overall temperature change

- c. The third point is that we use different size distributions for titania and sulfate. We chose the titania size distribution (r_m=0.045 µm, σ=1.8) from considering results of Pope et al (2012), namely that this is an optimised size distribution for a scattering aerosol. F11's size distribution (r_m=0.1 µm, σ=2.0) was selected from observations of natural mineral dust aerosols of which titania is a minor component. The key difference between these size distributions is the median radius, which is much smaller in our case, and therefore the titania aerosols in our simulations absorb and scatter short wave radiation more efficiently, hence more solar radiation is absorbed in the aerosol layer resulting in greater stratospheric heating.
  For sulfate, we took the *volc2* size distribution from Rasch et al (2008) (r_m=0.376 µm, σ=1.25) which is based on stratospheric aerosol observations in a post-volcanic period. Our Pinatubo simulations in section 3 show close conformity to observations. F11's sulfate size distribution (r_m=0.1 µm, σ=2.0) is much wider (i.e. their σ is greater). Therefore, while the effective radii of the distributions are comparable (0.43 and 0.33 respectively), F11 has more coarse particles that absorb efficiently in the long wave spectrum. Hence F11's sulfate has a greater stratospheric heating efficacy (i.e. heating per burden) than our sulfate, from more long wave absorption

- d. The fourth point is that our aerosol layer is much higher than F11's idealised aerosol layer. Whereas our aerosol concentrations peak at ~30 km altitude, F11's are evenly spaced between the tropopause and 22km altitude. Again, we have the advantage of accurate dynamical transport as we are using a 3-D global model

- e. For titania, F11 use the parallel refractive indices, from Ribarsky (1977) whilst we use an average of the parallel and perpendicular (or ordinary and extraordinary – denoting the polarisation of the scattered field). Angus Ferraro (personal communication) reports that, when re-running their FDH code with the perpendicular refractive indices instead of parallel, "the perpendicular refractive indices produce slightly stronger tropical heating"

Although points (a), (b), (d), and (e) will contribute to the difference in stratospheric temperatures (i.e. that our titania produces more warming, whilst their sulfate produces more warming), it is point (c) that is likely most important. We believe that

our chosen size-distributions are appropriate for the study here, as Pope et al (2012) try and maximise the impact of a specifically tailored TiO_2 aerosol. We therefore add the following paragraph to the discussion.

We find that sulfate induces less stratospheric warming than titania. In contrast, Ferraro et al (2011) found that the peak stratospheric warming for titania was 30% of that from sulfate. Although the different climatologies, model configurations, and aerosol spatial distributions will contribute to the difference in stratospheric temperature adjustment between our and Ferraro's work, the primary reason for the disparity is likely to be the aerosol size distributions. Our titania is smaller (median radius = 0.045 μm compared to 0.1 μm for Ferraro et al (2011)) and therefore scatters and absorbs SW more efficiently, producing a greater localised 'solar' warming. Their sulfate distribution contains a larger spread (σ = 2.0 for Ferraro et al (2011) compared to σ = 1.25 here), resulting in more coarse-mode particles and greater LW absorption. This disparity further highlights the sensitivity of climatic effects to the specified aerosol size distribution.

While we are comparing our work with Ferraro et al (2011), it is necessary to highlight major errors within their work that should be taken into account when comparing our results. In a personal communication, Angus Ferraro informed me that the aerosol density was not modified/ considered in either the calculation of the optical properties or the specification of the aerosol layer mass in their work. This is important - the specific absorption/ scattering coefficients plotted in their figure 1 are intrinsic properties; they depend on the density of the aerosol. The assumed density of 1000 kg/m^3 as used by Ferraro et al (2011) for calculation of all their aerosol's optical properties is not appropriate for either sulfate or titania, which should be represented by densities of ~1600 kg/m^3 and ~4000 kg/m^3. Consequently, the coefficients plotted for sulfate and titania in their figure 1 should be multiplied by 1/1.6 and 1/4 respectively to obtain realistic values. Similarly, the mass burdens given in their table 1 for sulfate and titania should be multiplied by 1.6 and 4 respectively to obtain appropriate values. This correction gives forcing efficiencies comparable to ours (see the table below). Should the disparity between the optical coefficients in our figure 1 and theirs be scrutinised, then this is the explanation. We have added the following to the above paragraph.

On a separate note, Ferraro et al (2011) neglected to alter the aerosol density component in the calculation of their aerosol masses and specific optical properties [A. Ferraro, personal communication]. The density that they used for all the aerosols of 1000 kg/m^3 is arguably applicable to black carbon, but not to sulfate and titania (which instead are ~1600 and ~4000 kg/m^3). Therefore, their aerosol burdens for sulfate and titania should be multiplied by 1.6 and 4 respectively, and their optical coefficients divided by 1.6 and 4, to obtain appropriate values.

Table T1	Sulfate		Titania	
	F11	This work	F11	This work
Burden (Tg)	14.5	49.5	3	20.2
Estimated Forcing (Wm^{-2})	3.5	8.5	3.5	8.5
Forcing efficiency (Wm^{-2}Tg^{-1})	0.24	0.17	1.17	0.42
Corrected burden (Tg)	23.2	49.5	12	20.2
Corrected forcing efficiency (Wm^{-2}Tg^{-1})	0.15	0.17	0.29	0.42

5. P30050 – The reviewer notes that the description we provide for our methods is insufficient. We appreciate that this aspect of the report is under-developed and would benefit from further detail. We therefore describe the exact methods used to obtain injection rates and conduct the simulations, in order that a reader would be able to reproduce these results.

Firstly, as noted by another reviewer, the top of the atmosphere radiative flux imbalance (hereafter *TOA-Imb*) is loosely defined in the report and requires further elaboration. To calculate the TOA-Imb for a certain simulation, we calculate the TOA net radiation (incoming SW minus outgoing LW+SW) and average this annually and globally (denote this value *R(t)* where *t* refers to the year). Next we do the same for each year of the 240-year perpetual pre-industrial control simulation. We then average these values to obtain the net radiative imbalance of the pre-industrial control simulation (denote this *C*). The TOA-Imb for year *t* is calculated as *R(t) – C*. The following has been added to the supplement to explain the method.
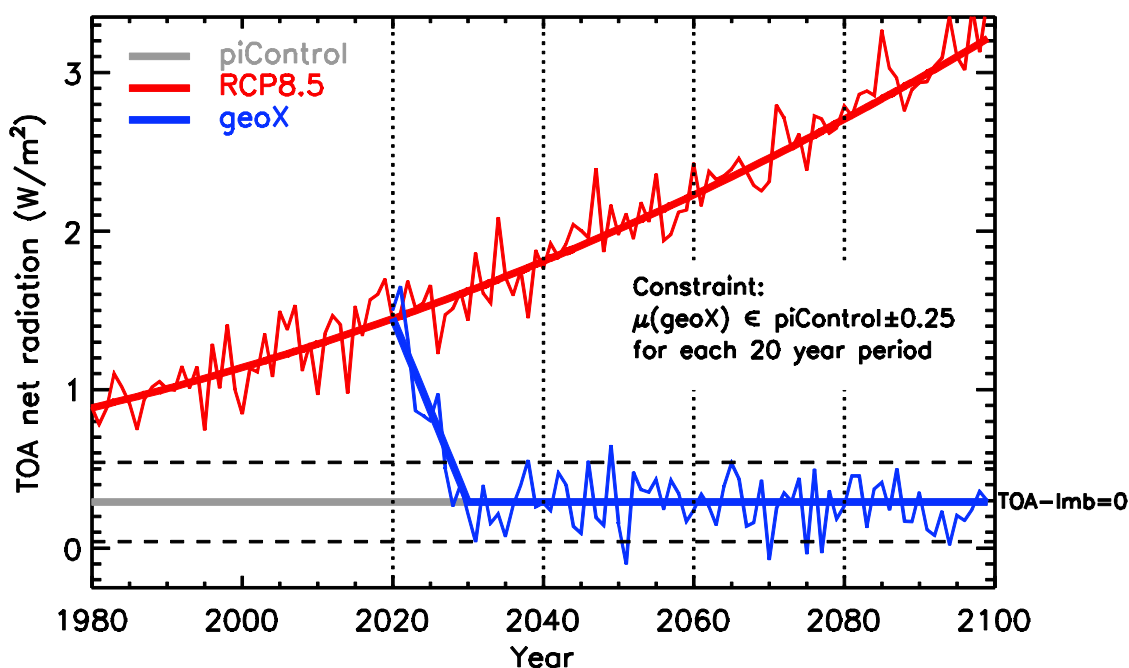

Fig. S2 *Schematic of the geoengineering experiment outline*

We now describe the simulation timeline. The RCP8.5 simulations had already been conducted prior to this investigation. The geoengineering simulations took place in 3 distinct phases: (a) we performed atmosphere-only simulations of 1Tg/yr aerosol injection to determine the aerosol TOA radiative effect; (b) we used the aerosol radiative effect to calculate initial injection rate estimates; (c) we began the 80-year GCM integrations, calibrating the injection rates *en route*.

a. We performed atmosphere-only simulations with a constant 1 Tg/yr aerosol injection rate using historical background-conditions (1990-2005). We then determined the steady-state annual/global-mean aerosol radiative effect (the difference in TOA net radiation between the aerosol simulation and the control), which is given in the following table. For sulfate, because the radiative effect was small, we performed an additional simulation with $5Tg[SO_2]/yr$ and then divided the results by 5 for precision. Similarly, the black carbon simulation failed to converge to steady state within 15 years and was therefore run for a further 15 years.

Table T2	Sulfate	Titania	Black Carbon
TOA radiative effect $(Wm^{-2} / Tg\ yr^{-1})$	0.46	1.1	7.4

b. Rather than use the TOA-Imb from the RCP8.5 simulations to estimate the required aerosol injection rates, we instead used the Anthropogenic Radiative Forcing (ARF), which was acquired from http://www.pik-potsdam.de/~mmalte/rcps/ (see Meinshausen et al, 2011). Specifically, we deducted the 1860 ARF ($0.17\ Wm^{-2}$) from the ARFs for 2020, 2040, 2060, 2080, and 2100, and then calculated the injection rates required to offset these adjusted ARFs by dividing by the TOA aerosol radiative effect. Because each model will have an ARF which is different from Meinshausen et al (2011) it is possible that our initial estimate is in error. However, our method uses this only as an initial 1st guess for the injection rates, which are iteratively adjusted as described in c). The model then linearly interpolates the injection rates between these years.

Table T3	Anthro-RF (Wm^{-2})		SO$_2$ injection rate (Tg/yr)		Titania injection rate (Tg/yr)		BC injection rate (Tg/yr)	
Year	Actual	Adjusted	Initial	Final	Initial	Final	Initial	Final
2020	2.56	2.39	5.2	4.4	2.2	1.4	0.32	0.21
2040	3.83	3.66	8.0	7.4	3.3	2.5	0.49	0.29
2060	5.34	5.17	11.2	11.6	4.7	4.1	0.70	0.45

2080	6.79	6.62	14.4	13.6	6.0	4.8	0.89	0.62
2100	8.15	7.98	17.4	14.2	7.3	6.2	1.08	0.88

    c. A single simulation was then initiated for each aerosol, with initial injection rates as specified in table T3. After every 20 year interval, the simulation was stopped and the TOA-Imb was calculated for that time period. If there was significant deviation from zero (we adopted |mean(TOA-Imb)|> 0.25 Wm^{-2} as the criterion), then we recalculated the amount of injection required. The recalibration was conducted as follows: the TOA-RF at the end of the 20 year period (time = t_{20}) was calculated for the mean of the RCP8.5 ensemble, denote this R_{rcp}. The injection of aerosol at time t_{20} at rate I_{geo} produced TOA-Imb R_{geo} which we wish to be zero. Therefore an improved injection rate at t_{20} would be $I'_{geo} = I_{geo} . R_{rcp}/(R_{rcp} - R_{geo})$. Additionally, at all specified timesteps after t_{20} ($t_n = t_{20}+20n$, $n = 1,...$), we modify the injection rate as such: $I'_{geo}(t_n) = I_{geo}(t_n) . R_{rcp}/(R_{rcp} - R_{geo})$. After resetting the injection rates, we restarted the simulation from the start of the last time period. Final injection rates are given in table T3. We then used the final injection rates to run two more ensemble members for each aerosol

We agree with the reviewer that it is important to include all of this information in our work so that our results are readily reproducible; therefore we have added this to the supplementary material. We will also the following sentence to section 3, to point the reader to the supplementary material for a detailed methodology.
A detailed description of our methods is provided in the supplementary material (section S2).

We add the following to our Methods section.
We inject aerosol at such a rate as to maintain the top-of-the-atmosphere (TOA) net radiation at piControl levels. Specifically, we define the TOA radiative flux Imbalance (TOA-Imb) as the annual/global-mean TOA net radiation (incoming SW minus outgoing LW+SW) minus the average TOA net radiation of the piControl period. By sufficient aerosol injection, we aim to maintain TOA-Imb=0. This scenario represents our interpretation of 'equal amount of geoengineering' for each aerosol. The advantage of returning net radiation to piControl levels (rather than completely equilibrating TOA fluxes) is that piControl had already been simulated comprehensively for CMIP5 (240 model-years), hence permitting robust statistics to be calculated. The TOA radiative imbalance is a metric that satellites are able to measure (e.g. CERES [L'Ecuyer et al, 2015] and EarthCare [Illingworth et al, 2015]), albeit with +/- 3 W/m^2 accuracy at present [Priestley et al, 2011; von Schuckmann et al., 2016]. Therefore our target could be applicable to an actual SAI scenario. In contrast, Radiative Forcing (RF) (the net

radiation perturbation at the tropopause from some external forcing, after stratospheric adjustment), cannot be directly measured by satellites and therefore it would be difficult to obtain a specified radiative forcing in an actual SAI scenario. Of course, other metrics could be chosen [e.g. MacMartin et al., 2013], with each metric having its only signal/noise characteristic.

6. P30057 – The reviewer notes that our analysis pertaining to the hydrological cycle is too inadequate. We have altered the sentences concerning the hydrological cycle to add clarity to our argument.
    Additionally, producing an equivalent top of the atmosphere radiative perturbation with a SW-absorbing aerosol such as BC (or to a lesser extent titania) compared to a SW-scattering aerosol such as sulfate, induces a comparatively greater SW forcing at the surface. Bala et al (2008) showed that reduced latent heat fluxes compensate for the SW reduction at the surface, instigating a deceleration of the hydrological cycle that is proportional to the magnitude of the SW reduction. This explains the greater reduction in precipitation exhibited by BC in figures 6-8.

7. P30058 – This query forms two separate parts: (a) what is the likelihood of the BC and titania aerosol being/ becoming hygroscopic? (b) And would this impact the results given here? We assess these questions and summarise our findings for addition to the manuscript.

    a. Firstly, for this analysis we will assume that mineral dust represents titania as this is the most apposite natural proxy [Ndour et al, 2008]. Mineral dust consists of 1-10% titania by mass depending on location [Ndour et al, 2008] and therefore is arguably suitable for this approximation. The chemical and physical attributes of atmospheric (or at least tropospheric) BC are comparatively well-known [Liu et al, 2013]. Koehler et al (2009) show that most atmospheric mineral dust exhibits low hygroscopicity ($\kappa \sim 0.03$) although larger particles ($r_m > 0.1$ µm) exhibit a similar hygroscopicity to similar sized sea-salt and ammonium sulfate aerosols. Liu et al (2013) show that atmospheric BC generally exhibits low hygroscopicity in its pure form ($g_F \sim 1.05$) but the inclusion of soluble contaminants such as secondary organics increases the hygroscopity ($g_F \sim 1.25$). Therefore, fresh BC and titania particles are likely to exhibit low hygroscopicity and cloud condensation activity, but in an aged form and when internally mixed with hygroscopic species their hygroscopic activity will increase.

    b. We apply the hygroscopic growth scheme used for sulfate [d' Almeida et al, 1991] to titania and BC, using the same size-distributions and properties as used in the article, in order to test the sensitivity of the optical properties to hygroscopicity. The 550nm absorption and scattering coefficients for BC are approximately similar for dry aerosol and at < 30% Relative Humidity (RH), but increase by 10% and 40% respectively at 50% RH. For titania, the 550 nm

absorption and scattering coefficients are also similar for dry mode and at <30% RH, but increase by 55% and 32% respectively at 50% RH.

To summarise, the hygroscopicity of the BC and titania aerosol would increase over time due to internal mixing with hygroscopic constituents and coagulation, the latter process resulting in larger particles that can act as cloud condensation nuclei (CCN). However, the low relative humidity of the stratosphere (~0.3% [SPARC, 2006]) would result in minimal hygroscopic growth, and therefore our results should not be significantly affected.

Observations have shown that fresh BC aerosol is predominantly hydrophobic, but the uptake of soluble contaminants (e.g. secondary organics) results in increased hygroscopicity [Liu et al, 2013]. Mineral dust, which contains 1-10% titania by mass [Ndour et al, 2008], exhibits low hygroscopicity for radii < 0.1 µm and similar growth to equivalently-sized sulfate aerosol thereafter [Koehler et al, 2009]. Although the historical stratospheric water vapor content is low (~4.2 ppmv in the tropical lower stratosphere during the HIST period), aerosol-induced stratospheric warming in the TTL would increase the specific humidity of air entering the stratosphere, therefore impacting hygroscopic growth.

8. P30059 – Thanks for the comment, we have added the Tang et al reference to this section.
   This work has already been started for titania by Tang et al [2014].

9. P30059 – We agree with the reviewer that this section is under-developed and with questionable applicability. The NIOSH recommendations refer to particles less than radius < 0.05 µm as 'ultrafine' and < 1.5 µm as 'fine'. For titania, NIOSH recommends time-weighted-average exposure limits of 0.3 mg/m^3 and 2.4 mg/m^3 respectively, allowing for a 10 hour day and 40 hour week. It is highly unlikely that titania injected in the ultrafine mode in the stratosphere will remain in the ultrafine mode until deposition. Therefore, we add the second NIOSH exposure recommendation for fine particles and a caveat.
   ... the USA's National Institute for Occupational Safety and Health (NIOSH) recommends maximum exposure limits of 0.3 mg m^{-3} for ultrafine titania particles (radius <0.05 µm) and 2.4 mg m^{-3} for fine particles (radius < 1.5 µm) [Dankovic et al, 2011]. After undergoing coagulation and ageing in the atmosphere, it is likely that the second exposure limit is more applicable to this work. In our simulations, the maximum 2090's near-surface air concentration of titania (e.g. Fig. 4) for land regions between 60°S-60°N is 254 ng/m^3, which is of the order of 10^2 less than the NIOSH 'fine-particle' exposure limit.

10. P30048 – Thanks for the comment - the units have been corrected.

11. P30052 – Thanks again, the TiO_2 deposition rate has been added (11 mg/m^2/yr).

References added to the manuscript

Ramaswamy et al, 2001; Peters et al, 2013; Kravitz et al., 2015; Dhomse et al., 2014; Pithan and Mauritsen, 2014; Schmidt et al., 2013; Dessler et al, 2013; Gettelman et al., 2010; Niemeier et al., 2013; Liu et al., 2013; Ndour et al., 2008; Koehler et al., 2009; Weisenstein et al., 2015; Tang et al., 2014; Davies et al., 2005; Bellouin et al., 2007; Priestley et al., 2011; L'Ecuyer et al., 2015; Illingworth et al., 2015; Haywood et al., 2011; MacMartin et al., 2013; von Schuckmann et al., 2016